APPLIED AND ENVIRONMENTAL MICROBIOLOGY, Sept. 2004, p. 5323–5330 Vol. 70, No. 9
0099-2240/04/$08.00+0 DOI: 10.1128/AEM.70.9.5323–5330.2004

Role of Hexose Transport in Control of Glycolytic Flux in *Saccharomyces cerevisiae*

Karin Elbing,[1]* Christer Larsson,[1] Roslyn M. Bill,[2] Eva Albers,[1] Jacky L. Snoep,[3] Eckhard Boles,[4] Stefan Hohmann,[5] and Lena Gustafsson[1]

Department of Chemistry and Bioscience-Molecular Biotechnology, Chalmers University of Technology,[1] and Department of Cell and Molecular Biology-Microbiology, Göteborg University,[5] Göteborg, Sweden; School of Life and Health Sciences, Aston University, Birmingham, United Kingdom[2]; Department of Biochemistry, University of Stellenbosch, Matieland, South Africa[3]; and Institut für Mikrobiologie, Johan Wolfgang Goethe-Universität Frankfurt, Frankfurt am Main, Germany[4]

Received 25 February 2004/Accepted 14 May 2004

The yeast *Saccharomyces cerevisiae* predominantly ferments glucose to ethanol at high external glucose concentrations, irrespective of the presence of oxygen. In contrast, at low external glucose concentrations and in the presence of oxygen, as in a glucose-limited chemostat, no ethanol is produced. The importance of the external glucose concentration suggests a central role for the affinity and maximal transport rates of yeast's glucose transporters in the control of ethanol production. Here we present a series of strains producing functional chimeras between the hexose transporters Hxt1 and Hxt7, each of which has distinct glucose transport characteristics. The strains display a range of decreasing glycolytic rates resulting in a proportional decrease in ethanol production. Using these strains, we show for the first time that at high glucose levels, the glucose uptake capacity of wild-type *S. cerevisiae* does not control glycolytic flux during exponential batch growth. In contrast, our chimeric Hxt transporters control the rate of glycolysis to a high degree. Strains whose glucose uptake is mediated by these chimeric transporters will undoubtedly provide a powerful tool with which to examine in detail the mechanism underlying the switch between fermentation and respiration in *S. cerevisiae* and will provide new tools for the control of industrial fermentations.

The ability of the yeast *Saccharomyces cerevisiae* to readily degrade sugars to ethanol and carbon dioxide (CO_2) has been utilized by humans for several thousands of years for the fermentation of alcoholic beverages and bread baking. *S. cerevisiae* ferments sugars even under aerobic conditions when the glucose concentration in the medium exceeds 0.8 mM (15, 48). This causes diauxic growth in aerobic batch cultures: once glucose is consumed, the ethanol is oxidized to CO_2 in a second, strictly respiratory growth phase. In contrast, at low external glucose concentrations and under aerobic conditions, for instance, during growth in glucose-limited chemostat cultures, ethanol is not produced and carbon dioxide is the main catabolic carbon product (37). Thus, depending on the conditions, glucose is catabolized either through full oxidation to CO_2 or respirofermentatively into CO_2 and ethanol (24). For certain industrial applications, aerobic ethanol formation is a substantial problem, because it lowers the yield of the desired product. An important example is the use of *S. cerevisiae* as a host for heterologous protein production, where maximizing protein yield is the primary objective. In this and other industrial processes where *S. cerevisiae* is the preferred biocatalyst, it is therefore desirable to control ethanol formation. This has recently been achieved by genetic manipulation of sugar uptake (31).

Despite more than a century of intensive research, fundamental aspects of the control of glycolytic metabolism and the key step of the partitioning of pyruvate toward fermentative and/or respiratory pathways are still poorly understood. Glucose transport, hexose phosphorylation, and phosphofructokinase and pyruvate kinase activities have all been proposed to play central roles in the control of glycolysis (3, 11, 12, 17, 29, 36, 41). However, individual or simultaneous overproduction of glycolytic enzymes resulted either in no increases in glycolytic flux or in only incremental increases (7, 19, 20, 42, 43). Furthermore, attempts to correlate glycolytic flux and/or capacity with enzyme levels under different physiological conditions have generally failed (25, 28, 46). This is likely because the control of glucose degradation is distributed over several different metabolic reactions (14, 43): glucose transport has been suggested to be one of the most important players in this context (17, 51).

In *S. cerevisiae,* hexoses are transported by facilitated diffusion via more than 20 different hexose transporters (Hxt), which display distinct affinities for glucose and are all members of the major facilitator superfamily (27, 35) In a null strain lacking all known hexose transporters, glucose consumption and transport activity are completely abolished (50). The transporters Hxt1 to Hxt4 plus Hxt6 and Hxt7 are most important for the uptake of glucose (5, 9, 10, 33, 39, 40). In addition, Hxt5, Hxt8 to -11, Hxt13 to -17, Gal2, and the maltose trans-

* Corresponding author. Mailing address: Department of Chemistry and Bioscience-Molecular Biotechnology, Chalmers University of Technology, Box 462, SE-405 30 Göteborg, Sweden. Phone: 46 31 773 25 81. Fax: 46 31 773 25 99. E-mail: Karin.Otterstedt@molbiotech.chalmers.se.

porters Agt1, Ydl247w, and Yjr160c are all able to transport glucose and, when ectopically produced, individually support growth in a strain lacking all other transporters (50). The different transporters exhibit low (K_m, 50 to 100 mM), intermediate (K_m, ca. 10 mM), and high (K_m, 1 to 2 mM) glucose affinity (1, 2, 38, 39); the expression of those genes depends on the glucose concentration in the medium. Thus, high glucose concentrations mediate the repression of genes encoding transporters with high and intermediate affinities, while at the same time expression of genes for low-affinity transporters is induced (5, 9, 23, 34, 49).

The development of a strain in which all Hxt's have been deleted, and which therefore does not take up any glucose, has opened up the possibility of manipulating the hexose uptake step and thereby steering glycolytic metabolism. We surmised that chimeric sugar transporters composed of parts of the low-affinity Hxt1 transporter and the high-affinity Hxt7 transporter could be used to develop a series of strains with decreased glycolytic fluxes and reduced or abolished ethanol formation. Indeed, the sole expression of each of our chimeric genes resulted in a series of strains with a gradually increased proportion of respiratory catabolism; one strain produced only negligible amounts of ethanol (31). Here we present the complete series of strains producing functional chimeras between the hexose transporters Hxt1 and Hxt7, displaying decreasing glycolytic rates and maximal to zero ethanol-producing capacity. These strains offer the possibility of elucidating how glucose uptake controls the rate of glycolysis at high extracellular glucose concentrations, which is the aim of the present study. We show that in wild-type cells growing at high glucose levels the uptake step has no control over the glycolytic rate, while the chimeric high-affinity Hxt transporters with decreased glucose uptake rates control the rate of glycolysis to a high degree.

MATERIALS AND METHODS

Yeast strains. All *S. cerevisiae* strains used were derived from the wild-type CEN.PK2-1C strain (*MAT***a** *leu2-3,112 ura3-52 trp1-289 his3-*Δ *MAL2-8*^{c} *SUC2 hxt17*Δ) (45). The auxotrophic markers *HIS3*, *TRP1*, *LEU2*, and *URA3* were reintroduced into the genome to generate strain KOY.PK2-1C83 (Table 1), without auxotrophic requirements. KOY.VW100 (31) was used to introduce the chimeric constructs and was made prototrophic by integration of *URA3*. Genotypes and chimeric constructs are given in Table 1.

Construction of chimeric hexose transporters. Chimeric hexose transporters were generated by the PCR overlap extension method (21). Each construct contained a portion of *HXT1* encoding the amino terminus of the transporter and a portion of *HXT7* encoding the carboxy terminus, with a fusion point within each of the 12 predicted transmembrane (TM) regions (Table 1). For amplification, plasmids pHXT1-2 (containing *HXT1*) (39) and p21 (containing *HXT7*) (40) were used. Constructs were integrated into the *HXT7* promoter cassette by recombination, replacing the *Kluyveromyces lactis URA3* marker, and transformants were selected on plates containing 5-fluoroorotic acid (5-FOA) (4). Transformants were first selected for functional glucose transport on plates containing 2% tryptone, 1% yeast extract, and 2% glucose and then incubated on plates containing 2% maltose, 5 g of ammonium sulfate liter^{-1}, 1.7 g of yeast nitrogen base without amino acids liter^{-1}, 120 mg of uracil liter^{-1}, and 0.1% 5-FOA to confirm the loss of *URA3*. *HXT1–HXT7* constructs that supported growth on glucose were amplified by PCR and sequenced. They were free from mutations with the exception of *TM6** (31) (see also Results) and *TM10*. Thus, *TM10* was excluded from further analysis due to the presence of several point mutations. Proteins Tm6 to Tm9 are considered nonfunctional, because no transformants were obtained on glucose plates.

Medium and cultivation in fermentors. Precultures were grown at 30°C and a rotation rate of 200 rpm for 24 h in 500-ml Erlenmeyer flasks (E-flasks) containing 50 ml of double-concentrated complete minimal medium (47). The *TM6** strain was grown for 48 h, because the growth rate was slow in E-flasks. For experimental fermentations, bioreactors (Chemap AG, Volketswil, Switzerland) containing 1.5 liters of double-concentrated complete minimal medium, 100 μl of polypropylene glycol P2000 (Sigma-Aldrich, Stockholm, Sweden) liter^{-1} as an antifoaming agent, and 2% glucose were inoculated to an optical density at 610 nm (OD_{610}) of 0.03 to 0.07. Conditions were kept constant at 30°C, 1,500 rpm, and pH 5.0. The gas flow was kept at 0.75 liter min^{-1} by using mass flow regulators (Bronkhorst, Ruurlo, The Netherlands), and the off gas was passed through a condenser to avoid evaporation. The performance of the culture was monitored continuously by measuring CO_2 production and oxygen (O_2) consumption by use of an acoustic carbon dioxide and oxygen monitor (type 1308; Brüel and Kjær, Nærum, Denmark). The respiratory quotient (RQ) of the culture was calculated as the ratio of the CO_2 production rate to the O_2 consumption rate.

Biochemical determinations. Dry weight was measured in duplicate by sedimenting 5 ml of cell culture twice at 2,313 × *g* for 5 min each time in preweighed dry glass tubes, washing the pellet once with 5 ml of deionized water (MilliQ), and drying for 24 h at 110°C before temperature equilibration and weighing. Glucose, maltose, ethanol, glycerol, and acetate concentrations in the growth medium were determined in culture supernatants (1 min at 16,060 × *g*) by using enzymatic combination kits (Roche Diagnostics, Bromma, Sweden).

Consumption and production rates. Glucose consumption and ethanol production rates were calculated by using several samples from the logarithmic-growth phase at glucose concentrations ranging from 8 to 20 g liter^{-1}. The mean value of the dry weight in the specific interval was used to determine the specific consumption and production rates.

Sugar uptake analysis. For sugar uptake determinations, an overnight preculture was used to inoculate 200 ml of complete minimal medium in 1-liter E-flasks. Cells were grown at 30°C and 200 rpm to logarithmic phase and were reinoculated in 1 liter of medium in 5-liter baffled E-flasks. Cells were harvested at an OD_{610} of 1.0, washed twice with 0.1 M potassium phosphate buffer (pH 6.5), diluted to a cell density of 7.5% (wt/vol), and kept on ice until uptake of [^{14}C]glucose (Amersham Life Science, Uppsala, Sweden) was assayed as described by Özcan and coworkers (32) with the modifications developed by Walsh and coworkers (49). Radioactivity was quantified by using a liquid scintillation detector (Beckman Coulter AB, Bromma, Sweden). Total cellular protein was determined by the Lowry method (26) with bovine serum albumin (Amersham Life Science) as a standard. Data from at least two independent experiments (performed in duplicate) were analyzed by using computer-assisted nonlinear regression. The calculations indicated one-component Michaelis-Menten uptake kinetics.

RESULTS

Construction of hexose transport chimeras. For the generation of chimeras, we chose Hxt1 and Hxt7 because they are the dominating transporters for glucose metabolism and display the lowest and highest glucose affinity, respectively (5). Hxt1 and Hxt7 each have 570 amino acids; they are 72% identical and are predicted to consist of 12 membrane-spanning domains, with the amino and carboxy termini located in the cytosol (23).

Different portions of the *HXT1* and *HXT7* genes were fused within the predicted TM region such that all chimeras consisted of a segment with the amino terminus of Hxt1 and the carboxy terminus of Hxt7 (Table 1). The constructs were integrated into the genome of the *hxt*-null strain KOY.VW100 (31) (Table 1) such that expression was under the control of the truncated, strong, and constitutive *HXT7* promoter (19). Subsequently, all auxotrophic markers were restored. generating prototrophic strains to avoid any influence on growth and metabolism by medium supplements. Twelve gene fusions were constructed in this way and named according to the number of the TM domain of the chimera where the fusion was made. For example, the prototrophic strain expressing the gene encoding the chimera fused in TM domain 1 was given the name KOY.TM1P and is referred to below as the *TM1* strain.

TABLE 1. Yeast strains used in this study

Strain	Genotype	Construct	Growth requirement	Source
KOY · PK2-1C83 (wild type)	*MAT***a** *MAL2-8^c SUC2*		Auxotrophic	K. D. Entian, Frankfurt am Main, Germany
			Prototrophic	K. Otterstedt (31)
KOY · VW100 (*hxt* null strain)	*MAT***a** *MAL2-8^c SUC2 hxt17Δ ura3-52 gal2Δ::loxP stl1Δ::loxP agt1Δ::loxP ydl247wΔ::loxP yjr160cΔ::loxP hxt13Δ::loxP hxt15Δ::loxP hxt16Δ::loxP hxt14Δ::loxP hxt12Δ::loxP hxt9Δ::loxP hxt11Δ::loxP hxt10Δ::loxP hxt8Δ::loxP hxt514Δ::loxP hxt2Δ::loxP hxt367Δ::loxP;* integration cassette at former *HXT367* site containing the truncated, constitutive promoter of *HXT7* (19), the *KIURA3* open reading frame for counter selection and the *HXT7* terminator		Auxotrophic	E. Boles (6, 50)
			Prototrophic	K. Otterstedt (31)
KOY · HXT1P	KOY · VW100 integration into cassette: *HXT7prom-HXT1-HXT7term ura3-52::URA3*		Prototrophic	This study
KOY · HXT7P	KOY · VW100 integration into cassette: *HXT7prom-HXT7-HXT7term ura3-52::URA3*		Prototrophic	This study
KOY · TM1P	KOY · VW100 integration into cassette: *HXT7prom-TM1-HXT7term ura3-52::URA3*	*TM1:HXT1*, bp 1–231; *HXT7*, bp 232–1713	Prototrophic	This study
KOY · TM2P	KOY · VW100 integration into cassette: *HXT7prom-TM2-HXT7term ura3-52::URA3*	*TM2:HXT1*, bp 1–391; *HXT7*, bp 392–1713	Prototrophic	This study
KOY · TM3P	KOY · VW100 integration into cassette: *HXT7prom-TM3-HXT7term ura3-52::URA3*	*TM3:HXT1*, bp 1–449; *HXT7*, bp 450–1713;	Prototrophic	This study
KOY · TM4P	KOY · VW100 integration into cassette: *HXT7prom-TM4-HXT7term ura3-52::URA3*	*TM4:HXT1*, bp 1–551; *HXT7*, bp 552–1713;	Prototrophic	This study
KOY · TM5P	KOY · VW100 integration into cassette: *HXT7prom-TM5-HXT7term ura3-52::URA3*	*TM5:HXT1*, bp 1–627; *HXT7*, bp 628–1713	Prototrophic	This study
KOY · TM6P[a]	KOY · VW100 integration into cassette: *HXT7prom-TM6-HXT7term ura3-52::URA3*	*TM6:HXT1*, bp 1–741; *HXT7*, bp 742–1713;		
KOY · TM6*P	KOY · VW100 integration into cassette: *HXT7prom-TM6*-HXT7term ura3-52::URA3*	*TM6*:HXT1*, bp 1–741; *HXT7*, bp 742–1713; C836A Scr279Tyr	Prototrophic	K. Otterstedt (31)
KOY · TM7P[a]	KOY · VW100 integration into cassette: *HXT7prom-TM7-HXT7term ura3-52::URA3*	*TM7:HXT1*, bp 1–1008; *HXT7*, bp 1009–1713	Prototrophic	This study
KOY · TM8P[a]	KOY · VW100 integration into cassette: *HXT7prom-TM8-HXT7term ura3-52::URA3*	*TM8:HXT1*, bp 1–1107; *HXT7*, bp 1108–1713	Prototrophic	This study
KOY · TM9P[a]	KOY · VW100 integration into cassette: *HXT7prom-TM9-HXT7term ura3-52::URA3*	*TM9:HXT1*, bp 1–1212; *HXT7*, bp 1213–1713	Prototrophic	This study
KOY · TM10P[b]	KOY · VW100 integration into cassette: *HXT7prom-TM10-HXT7term ura3-52::URA3*	*TM10:HXT1*, bp 1–1292; *HXT7*, bp 1293–1713	Prototrophic	This study
KOY · TM11P	KOY · VW100 integration into cassette: *HXT7prom-TM11-HXT7term ura3-52::URA3*	*TM11:HXT1*, bp 1–1437; *HXT7*, bp 1438–1713	Prototrophic	This study
KOY · TM12P	KOY · VW100 integration into cassette: *HXT7prom-TM12-HXT7term ura3-52::URA3*	*TM12:HXT1*, bp 1–1503; *HXT7*, bp 1504–1713	Prototrophic	This study

[a] Not able to grow on glucose.
[b] Excluded due to several mutations.

Strains producing proteins Tm6 to Tm9 were unable to grow in the presence of glucose, indicating that those chimeras were not functional glucose transporters. However, a mutated version of *TM6,* called *TM6**, in which serine 279 is replaced by tyrosine, mediated growth on glucose (31). Expression of genes encoding all other chimeras, i.e., Tm1 to Tm5 and Tm10 to Tm12, allowed growth on glucose (the *TM10* strain was omitted from further analysis because the chimera contained several mutations; see Materials and Methods).

General physiological characteristics. The physiology of the strains producing functional chimeras was examined in controlled aerobic batch cultures with 2% glucose as the sole carbon and energy source. For all but one strain, the CO_2 production and O_2 consumption profiles (Fig. 1) were typical for aerobic diauxic growth of *S. cerevisiae* on sugars (15). During the first respirofermentative phase, glucose was mainly catabolized fermentatively to CO_2, ethanol, glycerol, and minor by-products such as acetate (Fig. 1 and 2). In the subsequent respiratory phase, ethanol formed in the respirofermentative phase was respired almost completely to biomass as well as CO_2 and water. However, the chimera-producing strains exhibited a spectrum of physiological characteristics, with different proportions of the glucose being respired (Fig. 1 and 2). For this reason the RQ values, which were obtained from analysis of the gas curves during the respirofermentative glucose phase, ranged between 1.0 and 3.7 (Fig. 1). High RQ values indicate a predominantly fermentative metabolism, as exhibited by the wild-type, *TM11*, *TM12*, and *HXT1* strains. Values close to 1, as exhibited by the *TM4*, *TM5*, and *TM6** strains, suggest a largely or fully respiratory metabolism. The *HXT7*, *TM1*, *TM2*, and *TM3* strains all exhibited intermediate RQ values.

Carbon flux distribution. The highest ethanol yield (1.46 mol [mol of Glc]$^{-1}$) was obtained with the *HXT1* strain, which is one of the most pronounced fermentative strains, showing a high RQ and minor respiration. For the rest of the strains in

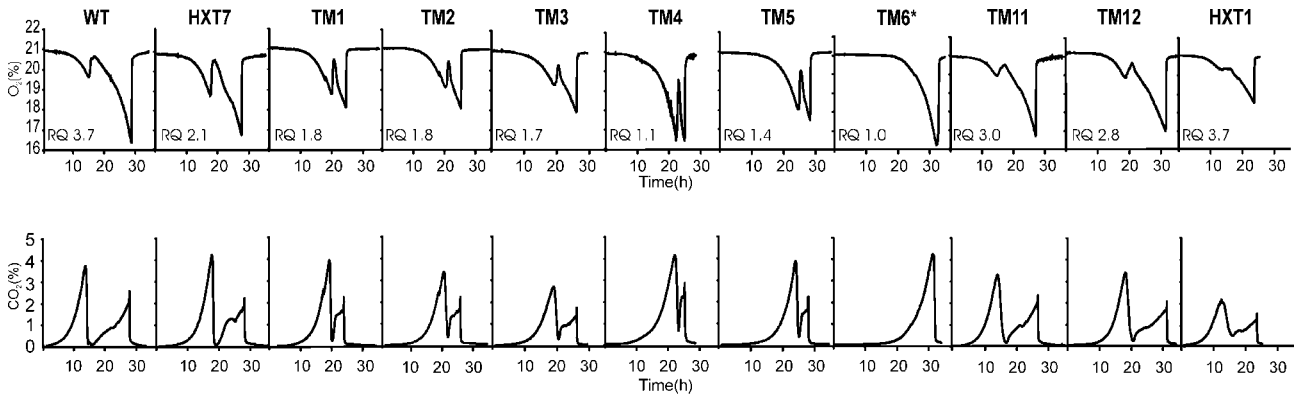

FIG. 1. Oxygen consumption and carbon dioxide production (both expressed as percentages) during aerobic batch cultivations, with glucose as the sole carbon and energy source, of the wild-type (WT), *HXT1*, *HXT7*, *TM1*, *TM2*, *TM3*, *TM4*, *TM5*, *TM6**, *TM11*, and *TM12* strains. Maximal RQ values in the glucose consumption phase were calculated from typical experiments.

the high-RQ group, namely, the wild-type, *TM11*, and *TM12* strains, the flow of glucose to respiration was minor (Fig. 2). This resulted in low biomass yields, in the range of 20 to 25 g (dry weight) (mol of Glc)$^{-1}$ (0.11 to 0.14 g [g of Glc]$^{-1}$) for the *TM11* and *TM12* strains. In contrast, growth of the *TM4*, *TM5*, and *TM6** strains, with RQ values close to 1, resulted in significantly higher biomass yields during the glucose phase (Fig. 2). The highest biomass yield of 61 g mol^{-1} (0.34 g [g of Glc]$^{-1}$) was obtained with the *TM6** strain. Since the C-molar biomass yield during respiration of glucose is higher than that during respiration of ethanol (8), the total biomass yield (including both glucose and ethanol catabolism) in the wild type reached only 54 g mol^{-1} (0.3 g [g of Glc]$^{-1}$).

Catabolic and anabolic flux rates. The strains exhibited different specific growth rates. The highest range (0.34 to 0.36 h^{-1}) was observed with the wild-type, *HXT1*, *HXT7*, *TM11*, and *TM12* strains, and the lowest was observed with the *TM6** strain (0.23 h^{-1}) (Table 2).

The genetically engineered strains formed clusters with similar glucose consumption and ethanol production rates. A linear correlation between the glucose consumption and ethanol production rates was observed (Fig. 3). Together with the wild type, the *HXT1*, *TM11*, and *TM12* strains displayed the highest glucose consumption rates, 14 to 18 mmol (g [dry weight])$^{-1}$ h^{-1}, and the highest ethanol production rates, 22 to 23 mmol (g [dry weight])$^{-1}$ h^{-1}. The lowest values were observed for the *TM4*, *TM5*, and *TM6** strains, with only 3.5 mmol (g [dry weight])$^{-1}$ h^{-1} of glucose consumption and no ethanol production for the *TM6** strain (31). As for RQ values, the *HXT7*, *TM1*, *TM2*, and *TM3* strains exhibited intermediate glucose consumption and ethanol production rates (Fig. 3).

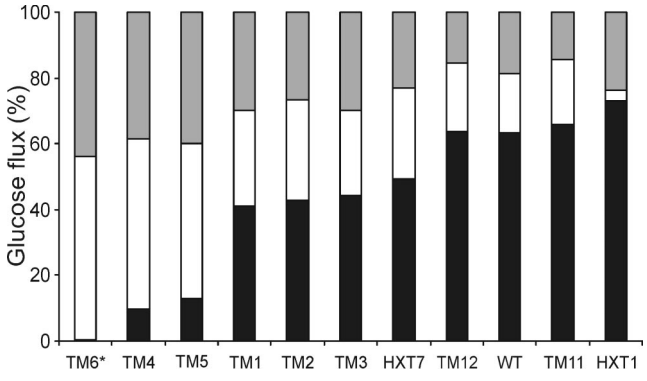

FIG. 2. Yield distributions based on carbon balance (expressed as percentages). See the legend to Fig. 1 for strain explanations. Solid bars, ethanol and carbon dioxide produced by fermentation; open bars, carbon dioxide produced by respiration plus glycerol and other by-products including acetate (calculated as the difference between the total amount of glucose consumed and that converted into ethanol, carbon dioxide, and biomass); shaded bars, biomass. All data were obtained during the maximal-production period in the respirofermentative glucose consumption phase for all strains except the *TM6** strain (which displays only a single phase).

Glucose uptake kinetics. The highest uptake capacities, exceeding 300 nmol (mg of protein)$^{-1}$ min^{-1}, were observed for the wild-type, *HXT1*, *TM11*, and *TM12* strains, while the rest of the strains, including *HXT7*, showed uptake capacities in the range of 35 to 130 nmol mg^{-1} min^{-1}. The *TM5* and *TM6** strains showed by far the lowest uptake capacities.

Glucose transport in the different strains exhibited low (K_m, 50 to 250 mM)- or medium- to high (K_m, ca. 2 to 10 mM)-affinity kinetics (Table 2). The differences in gas profiles (Fig. 1) correlated with the kinetic differences of the chimeric glucose transporters (Table 2). The strains producing proteins Tm1, -2, -3, -4, -5, and -6*, which are high-affinity transporters like Hxt7, utilized glucose at relatively high rates until a residual level of 1 to 5 mM glucose remained (data not shown; also Fig. 1, first minimum [O_2] or maximum [CO_2] in the gas curves). In contrast, the strains producing Tm11 and Tm12 together with the native Hxt1, which are low-affinity transporters, maintained high glucose consumption rates only until about 20 to 25 mM glucose remained in the medium (Fig. 1 and data not shown). The wild-type strain and strains producing high-affinity transporters displayed similar gas profiles during the diauxic shift. This behavior is expected, because the wild type induces expression of genes encoding high-affinity transporters toward the end of the respirofermentative phase (49).

For strains harboring the Hxt7-like transporters (Tm1 to Tm6*) as well as Hxt7 itself, the logarithm of the glucose consumption rate correlated linearly with the logarithm of the V_{app} (V_{max} corrected for the actual glucose concentration in the medium) for glucose transport (Fig. 4). However, the wild

TABLE 2. V_{max} and K_m of glucose transport and specific growth rates[a] of the wild-type, *HXT1, HXT7, TM1, TM2, TM3, TM4, TM5, TM6*, TM11,* and *TM12* strains

Relevant genotype	V_{max} of (nmol/mg of protein/min)	V_{max} (% of wild-type value)	K_m (mM)	μ (h^{-1})	μ (% of wild-type value)
Wild type	663 ± 31	100	76 ± 9.2	0.35	100
HXT1	806 ± 140	122	250 ± 74	0.34	97
TM12	302 ± 13	46	44 ± 4.3	0.35	100
TM11	522 ± 47	79	72 ± 4.0	0.36	103
HXT7	125 ± 7.6	19	2.5 ± 0.6	0.34	97
TM1	73 ± 5.2	11	4.6 ± 1.3	0.30	86
TM2	113 ± 3.1	17	7.0 ± 0.7	0.30	86
TM3	129 ± 5.6	19	6.2 ± 1.4	0.28	80
TM4	103 ± 7.0	16	7.6 ± 2.1	0.26	74
TM5	35 ± 1.9	5	4.9 ± 0.9	0.27	77
*TM6**	61 ± 2.1	9	3.5 ± 0.5	0.23	66

[a] Specific-growth-rate values were calculated during the respirofermentative phase. The specific growth rate of the *TM6** strain, which shows only one phase, was determined during respiratory metabolism.

type deviated from this correlation, and the low-affinity transporter strains (the *HXT1*, *TM11*, and *TM12* strains) are on the border of the correlation.

Metabolic control analysis. The use of our strains with altered glucose transport capacity offers the possibility to study the control of glycolytic flux by glucose uptake. By using log-log plots according to the theory of metabolic control analysis, it is possible to determine to what extent an enzymatic step controls the steady-state rate of a pathway (13, 20, 22). However, neither V_{max} nor V_{app} (Fig. 4) activities of the chimeric transporters can be used directly in an estimation of the control of glucose transport in wild-type *S. cerevisiae*. This is because the transporters not only have different V_{max} values but also have

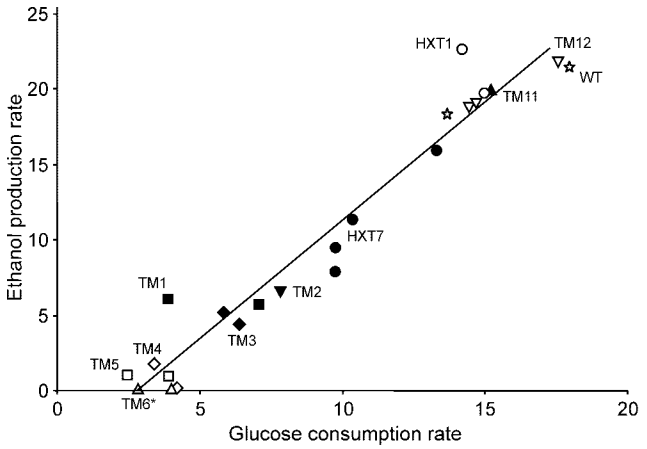

FIG. 3. Plot of the maximal specific ethanol production rate (expressed as millimoles of ethanol per gram [dry weight] per hour) versus the maximal specific glucose consumption rate (expressed as millimoles of glucose per gram [dry weight] per hour) of independent batches for the wild-type (WT) (open star), *HXT1* (open circles), *HXT7* (solid circles), *TM1* (solid squares), *TM2* (solid inverted triangles), *TM3* (solid diamonds), *TM4* (open diamonds), *TM5* (open squares), *TM6** (open triangles), *TM11* (solid triangles), and *TM12* (open inverted triangles) strains. All data were obtained during the maximal production period in the respirofermentative phase for all strains except the *TM6** strain (which displays only a single phase).

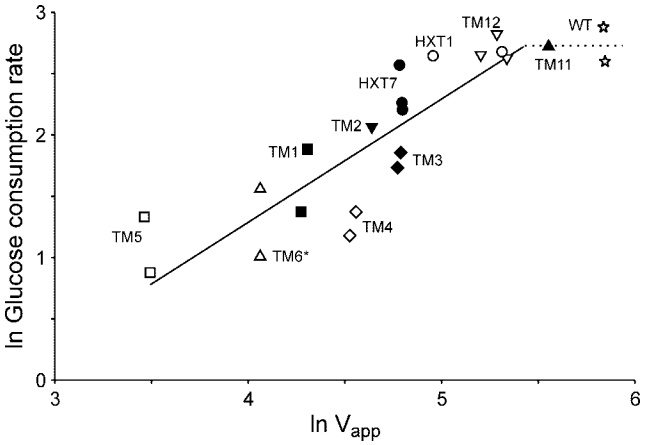

FIG. 4. Double logarithmic plot of the maximum specific glucose consumption rate (expressed as millimoles of glucose per gram [dry weight] per hour) versus the apparent glucose uptake rate (V_{app}, expressed as nanomoles of glucose per milligram of protein per minute). For strain and symbol explanations, see the legend to Fig. 3. All data were calculated during the respirofermentative phase, except for the *TM6** strain (which displays only a single phase).

different affinities (K_m) for glucose (see Table 2). Consequently, in order to use the chimeras for determination of the flux control of glucose transport in the wild-type strains, the V_{max} values of the different chimeras had to be adjusted such that they reflected the wild-type V_{max} under the actual conditions used. To do this, we calculated the corresponding wild-type V_{max} to obtain the flux observed in the chimera with given external and internal glucose concentrations (V_{adj}). To calculate the internal glucose concentration, it was assumed that glucose transport can be described by a symmetrical carrier model (44). However, when this equation was used with the V_{max}, K_m, and glucose consumption rates determined, negative intracellular glucose concentrations were obtained, as has also been reported previously (44). To overcome this difficulty, we performed our analysis by assuming that the internal glucose concentrations range from 0 to 3 mM, reflecting the lowest and highest reported values (44). Using this range of intracellular glucose concentrations and the extracellular glucose concentration at which the flux is determined, we could calculate V_{adj} (adjusted V_{max}). Below is a schematic explanation of how the maximal rate coefficients (V_{max}) of the chimeric strains were recalculated to wild-type activities, which were used in the control analysis.

$$f\left(K_m^{Chim}, V_{\max}^{Chim}, Glc_o, Glc_i\right) = V_{zero\text{-}trans}^{Chim}$$

$$f\left(V_{zero\text{-}trans}^{Chim}, K_m^{WT}, Glc_o, Glc_i\right) = V_{adj}^{Chim}$$

where Glc_o and Glc_i are extra- and intracellular glucose concentrations, respectively, $V_{zero-trans}$ is the zero-*trans* influx rate, and kinetic constants with superior "Chim" or "WT" are the kinetic constants for the chimera or the wild type, respectively. Below is the full rate equation used to convert the chimeric V_{max} into V_{adj} (44).

$$V_{adj}^{Chim}\frac{(Glc_o - Glc_i)}{K_m^{WT} + Glc_o + Glc_i + 0.91\dfrac{Glc_o\,Glc_i}{K_m^{WT}}}$$

$$= V_{max}^{Chim}\frac{(Glc_o - Glc_i)}{K_m^{Chim} + Glc_o + Glc_i + 0.91\dfrac{Glc_o\,Glc_i}{K_m^{Chim}}}$$

We verified this method of adjusting the V_{max} at different intracellular glucose levels by using a core model consisting of two reactions, i.e., the glucose transporter reaction and the rest of the metabolic reactions grouped together, the latter being described by an irreversible Michaelis-Menten equation. With this model we simulated the effect of varying the wild-type transporter and compared the results that would be observed in chimeras by using the method of adjusting the V_{max} as described above at different internal glucose concentrations. At an internal glucose concentration of zero, the model simulations gave identical results when the V_{max} for the chimeras was adjusted and when the wild-type V_{max} was changed. Only at high internal glucose concentrations (2 mM) could a significant difference be observed between simulations of the wild type and of chimeras, and then only for the high-affinity transporters (data not shown). These studies with the core model indicate that our approach of using internal glucose concentrations between 0 and 3 mM is correct. Generally, only a small effect is observed for the internal glucose concentration, and then only for the high-affinity chimeric enzymes. Thus, we used the V_{adj} values of the chimeric enzymes for our metabolic control analysis of transport in wild-type *S. cerevisiae*.

In a double-logarithmic plot of glycolytic flux, i.e., glucose consumption rate, and transport activity (V_{adj}), all strains except the wild-type and *TM11* strains followed a linear trend, with slopes of 1.07, 0.93, 0.83, and 0.75 (R^2 = 0.81, 0.78, 0.71, and 0.65, respectively) for intracellular glucose levels of 0, 1, 2, and 3 mM, respectively (see also Fig. 5). The slope in a log-log plot of flux against activity gives the flux control coefficient of the glucose transporter, and a value close to 1 indicates full control of the flux by the enzyme. Thus, the data in Fig. 5 show that the glucose transport step does not have high control at wild-type levels of transport activity. However, the transport step gains high control over glycolytic flux at 56% of the wild-type uptake rate.

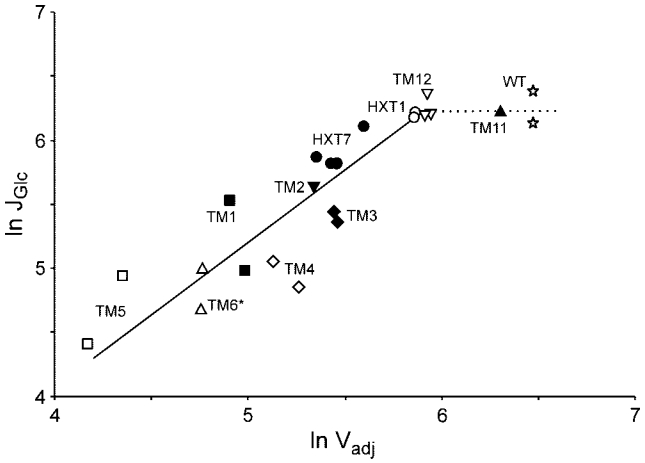

FIG. 5. Double-logarithmic plot of glycolytic flux, J_{Glc} (maximum specific glucose consumption rate, expressed as nanomoles of glucose per milligram of protein per minute) versus adjusted glucose transport activity, V_{adj} (expressed as nanomoles per milligram of protein per minute). The protein content was assumed to be 0.5 g (g [dry weight])$^{-1}$, and the intracellular glucose concentration was assumed to be 0 mM. For strain and symbol explanations, see the legend to Fig. 3. Values for all strains except the *TM6** strain (which displays only a single phase) were calculated during the respirofermentative phase.

DISCUSSION

We have constructed functional chimeras between the low- and high-affinity transporters Hxt1 and Hxt7 in order to further understand how changes in glucose uptake affect yeast metabolism. Our series of strains displayed different rates of ethanol production, which correlated linearly with the maximal specific glucose consumption rates attained during exponential growth on glucose (Fig. 3). Hence, restricted glucose consumption, and consequently a reduced glycolytic rate, is a strong candidate for explaining the observed differences in ethanol yield. Restricted glucose consumption, in turn, is explained by different capacities of the glucose transporters. Indeed, the strains with the highest glucose uptake capacity (V_{max} [Table 2], V_{app} [Fig. 4]) showed the highest glucose consumption and ethanol production rates, and vice versa. These observations are in line with earlier studies on *S. cerevisiae* (16, 32, 39, 51) and the dairy yeast *K. lactis* (18) in which sugar uptake appeared to be limiting fermentative growth, thereby causing respiratory utilization of sugars. Furthermore, the decreased glucose consumption rate seen in the *TM6** strain triggers a 4.5-times-higher respiratory rate (31), which might contribute to the low ethanol yield observed. The difference in respiratory rate between the *TM6** strain and the wild type amounts to an increased respiration capacity of 0.83 mmol of glucose $g^{-1}\,h^{-1}$ for the *TM6** strain. This is as much as 20% of the total glucose flux in the *TM6** strain.

Extrapolating the correlation in Fig. 3 to an ethanol production rate of zero points to a glucose consumption rate of 3 mmol (g [dry weight])$^{-1}\,h^{-1}$. This value, therefore, seems to be the highest rate possible without any ethanol production. Interestingly, approximately the same value can be extrapolated from data measured for strains with engineered galactose metabolism (Fig. 3 in reference 30) as well as for chemostat cultures at the onset of ethanol formation (9). The *TM6** strain seems to achieve precisely the highest rate of glucose consumption, allowing a fully respiratory catabolism.

The differences in the kinetic properties of the chimeric enzymes made it possible to estimate the control of glycolytic flux by glucose transport in wild-type *S. cerevisiae* during exponential growth at high levels of glucose. For the estimate, we have used the methodology of metabolic control analysis, which offers the possibility of determining to what extent an enzymatic step affects the total steady-state rate of a pathway (i.e., flux) (13, 20, 22): in our case, the control of glycolytic flux by the hexose transport step. The chimeric transporters constructed in this study showed transport activities ranging from 122 to 5% of wild-type activity (Table 2). According to Fig. 4,

a correlation between the glucose consumption rate and the apparent glucose transport capacity (V_{app}) was found. However, in order to properly estimate the control of glycolytic flux by glucose transport in wild-type cells, the V_{max} (or V_{app}) activities of the chimeric transporters cannot be used directly, because the transporters not only differ in V_{max} but also have different affinities (K_m) for glucose. Thus, as described in Results, the V_{max} values were recalculated to adjusted values (V_{adj}) by taking into account the affinities of the chimeras relative to the affinity of the wild type, as well as the influence of intracellular glucose. The results show that at low glucose transport activities, the glucose transporter has a high flux control, as reflected from the slope in Fig. 5, with a value close to 1. However at wild-type activities, such a correlation between transport activity and glycolytic flux is no longer present. The strains producing the transporter Hxt1 or Tm12 seem to perform at the limit where glucose transport loses this control. Thus, from our experiments, it appears as if the transporter has no or very low control over glycolytic flux in the wild type at high glucose concentrations.

A similar type of study on the control of glycolytic flux by glucose transport has been described previously for *Saccharomyces bayanus* (11). Here the cells were harvested at the diauxic shift, and the inhibitory effects of maltose and different extracellular glucose levels were used to manipulate the glucose transport activity. This study showed that the transport step exerted full control over glycolytic flux, with a flux control coefficient of 1.04 for the whole range of fluxes and uptake activities investigated. The explanation for the high flux control coefficient over the whole range in this study is that cells originating from the diauxic shift express the high-affinity uptake system, which, in line with the findings of our study, is expected to exert high control over the rate of glycolysis.

To conclude, we have shown that glucose transport can play a dominant role in controlling the flux of glycolysis even at high external glucose concentrations, if the transport capacity is reduced. However, it should be pointed out that during batch cultivation of the wild type on a 2% glucose medium, glucose transport has very little, if any, control over the glycolytic rate. In addition, our strains with different glycolytic rates offer both academic and industrial researchers a unique set of tools with which to dissect the partitioning between respiration and fermentation, as well as the regulation of glucose repression and derepression in *S. cerevisiae* at high extracellular glucose concentrations.

ACKNOWLEDGMENTS

We acknowledge the financial support of the Commission of the European Union via contract BIO4-CT98-0562, the Swedish National Energy Administration (P1009-5), the Swedish Council for Forestry and Agricultural Research (52.0609/97), and the Swedish Research Council (621-2001-1988) (to L.G.). S.H.'s position as researcher is supported by the Swedish Research Council. E.A. acknowledges a grant from the Knut and Alice Wallenberg Foundation. R.M.B. acknowledges financial support from the Commission of the European Union.

REFERENCES

1. **Bisson, L. F., D. M. Coons, A. L. Kruckeberg, and D. A. Lewis.** 1993. Yeast sugar transporters. Crit. Rev. Biochem. Mol. Biol. **28:**259–308.
2. **Bisson, L. F., and D. G. Fraenkel.** 1983. Involvement of kinases in glucose and fructose uptake by *Saccharomyces cerevisiae.* Proc. Natl. Acad. Sci. USA **80:**1730–1734.
3. **Blazquez, M. A., R. Lagunas, C. Gancedo, and J. M. Gancedo.** 1993. Trehalose-6-phosphate, a new regulator of yeast glycolysis that inhibits hexokinases. FEBS Lett. **329:**51–54.
4. **Boeke, J. D., F. LaCroute, and G. R. Fink.** 1984. A positive selection for mutants lacking orotidine-5′-phosphate decarboxylase activity in yeast: 5-fluoro-orotic acid resistance. Mol. Gen. Genet. **197:**345–346.
5. **Boles, E., and C. P. Hollenberg.** 1997. The molecular genetics of hexose transport in yeasts. FEMS Microbiol. Rev. **21:**85–111.
6. **Buziol, S., J. Becker, A. Baumeister, S. Jung, K. Mauch, M. Reuss, and E. Boles.** 2002. Determination of in vivo kinetics of the starvation-induced Hxt5 glucose transporter of *Saccharomyces cerevisiae*. FEM Yeast Res. **2:**283–291.
7. **Davies, S. E., and K. M. Brindle.** 1992. Effects of overexpression of phosphofructokinase on glycolysis in the yeast *Saccharomyces cerevisiae.* Biochemistry **31:**4729–4735.
8. **de Jong-Gubbels, P., P. Vanrolleghem, S. Heijnen, J. P. van Dijken, and J. T. Pronk.** 1995. Regulation of carbon metabolism in chemostat cultures of *Saccharomyces cerevisiae* grown on mixtures of glucose and ethanol. Yeast **11:**407–418.
9. **Diderich, J. A., M. Schepper, P. van Hoek, M. A. Luttik, J. P. van Dijken, J. T. Pronk, P. Klaassen, H. F. Boelens, M. J. de Mattos, K. van Dam, and A. L. Kruckeberg.** 1999. Glucose uptake kinetics and transcription of HXT genes in chemostat cultures of *Saccharomyces cerevisiae.* J. Biol. Chem. **274:**15350–15359.
10. **Diderich, J. A., J. M. Schuurmans, M. C. Van Gaalen, A. L. Kruckeberg, and K. Van Dam.** 2001. Functional analysis of the hexose transporter homologue HXT5 in *Saccharomyces cerevisiae.* Yeast **18:**1515–1524.
11. **Diderich, J. A., B. Teusink, J. Valkier, J. Anjos, I. Spencer-Martins, K. van Dam, and M. C. Walsh.** 1999. Strategies to determine the extent of control exerted by glucose transport on glycolytic flux in the yeast *Saccharomyces bayanus*. Microbiology **145:**3447–3454.
12. **Ernandes, J. R., C. De Meirsman, F. Rolland, J. Winderickx, J. de Winde, R. L. Brandao, and J. M. Thevelein.** 1998. During the initiation of fermentation overexpression of hexokinase PII in yeast transiently causes a similar deregulation of glycolysis as deletion of Tps1. Yeast **14:**255–269.
13. **Fell, D. A.** 1992. Metabolic control analysis: a survey of its theoretical and experimental development. Biochem. J. **286:**313–330.
14. **Fell, D. A., and S. Thomas.** 1995. Physiological control of metabolic flux: the requirement for multisite modulation. Biochem. J. **311:**35–39.
15. **Fiechter, A., G. F. Fuhrmann, and O. Kappeli.** 1981. Regulation of glucose metabolism in growing yeast cells. Adv. Microb. Physiol. **22:**123–183.
16. **Gamo, F. J., M. J. Lafuente, and C. Gancedo.** 1994. The mutation DGT1–1 decreases glucose transport and alleviates carbon catabolite repression in *Saccharomyces cerevisiae.* J. Bacteriol. **176:**7423–7429.
17. **Gancedo, C., and R. Serrano.** 1989. Energy-yielding metabolism, 2nd ed., vol. 3. Academic Press, London, England.
18. **Goffrini, P., I. Ferrero, and C. Donnini.** 2002. Respiration-dependent utilization of sugars in yeasts: a determinant role for sugar transporters. J. Bacteriol. **184:**427–432.
19. **Hauf, J., F. K. Zimmermann, and S. Muller.** 2000. Simultaneous genomic overexpression of seven glycolytic enzymes in the yeast *Saccharomyces cerevisiae.* Enzyme Microb. Technol. **26:**688–698.
20. **Heinisch, J.** 1986. Isolation and characterization of the two structural genes coding for phosphofructokinase in yeast. Mol. Gen. Genet. **202:**75–82.
21. **Ho, S. N., H. D. Hunt, R. M. Horton, J. K. Pullen, and L. R. Pease.** 1989. Site-directed mutagenesis by overlap extension using the polymerase chain reaction. Gene **77:**51–59.
22. **Kacser, H., and J. A. Burns.** 1973. The control of flux. Symp. Soc. Exp. Biol. **27:**65–104.
23. **Kruckeberg, A. L.** 1996. The hexose transporter family of *Saccharomyces cerevisiae.* Arch. Microbiol. **166:**283–292.
24. **Larsson, C., A. Blomberg, and L. Gustafsson.** 1991. Use of microcalorimetric monitoring in establishing continuous energy balances and in continuous determinations of substrate and product concentrations of batch-grown *Saccharomyces cerevisiae.* Biotechnol. Bioeng. **38:**447–458.
25. **Larsson, C., A. Nilsson, A. Blomberg, and L. Gustafsson.** 1997. Glycolytic flux is conditionally correlated with ATP concentration in *Saccharomyces cerevisiae*: a chemostat study under carbon- or nitrogen-limiting conditions. J. Bacteriol. **179:**7243–7250.
26. **Lowry, O. H., N. J. Rosebrough, A. L. Farr, and R. J. Randall.** 1951. Protein measurement with the Folin phenol reagent. J. Biol. Chem. **193:**265–275.
27. **Marger, M. D., and M. H. Saier, Jr.** 1993. A major superfamily of transmembrane facilitators that catalyse uniport, symport and antiport. Trends Biochem. Sci. **18:**13–20.
28. **Nissen, T. L., U. Schulze, J. Nielsen, and J. Villadsen.** 1997. Flux distributions in anaerobic, glucose-limited continuous cultures of *Saccharomyces cerevisiae.* Microbiology **143:**203–218.
29. **Oehlen, L. J., M. E. Scholte, W. de Koning, and K. van Dam.** 1994. Decrease in glycolytic flux in *Saccharomyces cerevisiae* cdc35–1 cells at restrictive temperature correlates with a decrease in glucose transport. Microbiology **140:**1891–1898.
30. **Ostergaard, S., L. Olsson, M. Johnston, and J. Nielsen.** 2000. Increasing

galactose consumption by *Saccharomyces cerevisiae* through metabolic engineering of the *GAL* gene regulatory network. Nat. Biotechnol. **18:**1283–1286.
31. **Otterstedt, K., C. Larsson, R. M. Bill, A. Stahlberg, E. Boles, S. Hohmann, and L. Gustafsson.** 2004. Switching the mode of metabolism in the yeast *Saccharomyces cerevisiae.* EMBO Rep. **5:**532–537.
32. **Ozcan, S., K. Freidel, A. Leuker, and M. Ciriacy.** 1993. Glucose uptake and catabolite repression in dominant HTR1 mutants of *Saccharomyces cerevisiae.* J. Bacteriol. **175:**5520–5528.
33. **Ozcan, S., and M. Johnston.** 1999. Function and regulation of yeast hexose transporters. Microbiol. Mol. Biol. Rev. **63:**554–569.
34. **Ozcan, S., and M. Johnston.** 1995. Three different regulatory mechanisms enable yeast hexose transporter (*HXT*) genes to be induced by different levels of glucose. Mol. Cell. Biol. **15:**1564–1572.
35. **Pao, S. S., I. T. Paulsen, and M. H. Saier, Jr.** 1998. Major facilitator superfamily. Microbiol. Mol. Biol. Rev. **62:**1–34.
36. **Pearce, A. K., K. Crimmins, E. Groussac, M. J. Hewlins, J. R. Dickinson, J. Francois, I. R. Booth, and A. J. Brown.** 2001. Pyruvate kinase (Pyk1) levels influence both the rate and direction of carbon flux in yeast under fermentative conditions. Microbiology **147:**391–401.
37. **Postma, E., W. A. Scheffers, and J. P. van Dijken.** 1989. Kinetics of growth and glucose transport in glucose-limited chemostat cultures of *Saccharomyces cerevisiae* CBS 8066. Yeast **5:**159–165.
38. **Ramos, J., K. Szkutnicka, and V. P. Cirillo.** 1988. Relationship between low- and high-affinity glucose transport systems of *Saccharomyces cerevisiae.* J. Bacteriol. **170:**5375–5377.
39. **Reifenberger, E., E. Boles, and M. Ciriacy.** 1997. Kinetic characterization of individual hexose transporters of *Saccharomyces cerevisiae* and their relation to the triggering mechanisms of glucose repression. Eur. J. Biochem. **245:** 324–333.
40. **Reifenberger, E., K. Freidel, and M. Ciriacy.** 1995. Identification of novel *HXT* genes in *Saccharomyces cerevisiae* reveals the impact of individual hexose transporters on glycolytic flux. Mol. Microbiol. **16:**157–167.
41. **Reijenga, K. A., J. L. Snoep, J. A. Diderich, H. W. van Verseveld, H. V. Westerhoff, and B. Teusink.** 2001. Control of glycolytic dynamics by hexose transport in *Saccharomyces cerevisiae.* Biophys. J. **80:**626–634.
42. **Rosenzweig, R. F.** 1992. Regulation of fitness in yeast overexpressing glycolytic enzymes: parameters of growth and viability. Genet. Res. **59:**35–48.
43. **Schaaff, I., J. Heinisch, and F. K. Zimmermann.** 1989. Overproduction of glycolytic enzymes in yeast. Yeast **5:**285–290.
44. **Teusink, B., J. A. Diderich, H. V. Westerhoff, K. van Dam, and M. C. Walsh.** 1998. Intracellular glucose concentration in derepressed yeast cells consuming glucose is high enough to reduce the glucose transport rate by 50%. J. Bacteriol. **180:**556–562.
45. **van Dijken, J. P., J. Bauer, L. Brambilla, P. Duboc, J. M. Francois, C. Gancedo, M. L. Giuseppin, J. J. Heijnen, M. Hoare, H. C. Lange, E. A. Madden, P. Niederberger, J. Nielsen, J. L. Parrou, T. Petit, D. Porro, M. Reuss, N. van Riel, M. Rizzi, H. Y. Steensma, C. T. Verrips, J. Vindelov, and J. T. Pronk.** 2000. An interlaboratory comparison of physiological and genetic properties of four *Saccharomyces cerevisiae* strains. Enzyme Microb. Technol. **26:**706–714.
46. **van Hoek, P., J. P. van Dijken, and J. T. Pronk.** 2000. Regulation of fermentative capacity and levels of glycolytic enzymes in chemostat cultures of *Saccharomyces cerevisiae.* Enzyme Microb. Technol. **26:**724–736.
47. **Verduyn, C., E. Postma, W. A. Scheffers, and J. P. Van Dijken.** 1992. Effect of benzoic acid on metabolic fluxes in yeasts: a continuous-culture study on the regulation of respiration and alcoholic fermentation. Yeast **8:**501–517.
48. **Verduyn, C., T. P. L. Zomerdijk, J. P. Van Dijken, and W. A. Scheffers.** 1984. Continuous measurement of ethanol production by aerobic yeast suspension with an enzyme electrode. Appl. Microbiol. Biotechnol. **19:**181–185.
49. **Walsh, M. C., H. P. Smits, M. Scholte, and K. van Dam.** 1994. Affinity of glucose transport in *Saccharomyces cerevisiae* is modulated during growth on glucose. J. Bacteriol. **176:**953–958.
50. **Wieczorke, R., S. Krampe, T. Weierstall, K. Freidel, C. P. Hollenberg, and E. Boles.** 1999. Concurrent knock-out of at least 20 transporter genes is required to block uptake of hexoses in *Saccharomyces cerevisiae.* FEBS Lett. **464:**123–128.
51. **Ye, L., A. L. Kruckeberg, J. A. Berden, and K. van Dam.** 1999. Growth and glucose repression are controlled by glucose transport in *Saccharomyces cerevisiae* cells containing only one glucose transporter. J. Bacteriol. **181:** 4673–4675.